



HAL
open science

Structural control in micelles of alkyl acrylate-acrylate copolymers via alkyl chain length and block length

Özge Azeri, Dennis Schönfeld, Laurence Noirez, Michael Gradzielski

► **To cite this version:**

Özge Azeri, Dennis Schönfeld, Laurence Noirez, Michael Gradzielski. Structural control in micelles of alkyl acrylate-acrylate copolymers via alkyl chain length and block length. *Colloid and Polymer Science*, 2020, 298, pp.829 - 840. 10.1007/s00396-020-04663-y . hal-03028485

HAL Id: hal-03028485

<https://hal.science/hal-03028485>

Submitted on 7 Dec 2020

HAL is a multi-disciplinary open access archive for the deposit and dissemination of scientific research documents, whether they are published or not. The documents may come from teaching and research institutions in France or abroad, or from public or private research centers.

L'archive ouverte pluridisciplinaire **HAL**, est destinée au dépôt et à la diffusion de documents scientifiques de niveau recherche, publiés ou non, émanant des établissements d'enseignement et de recherche français ou étrangers, des laboratoires publics ou privés.

Structural Control in Micelles of Alkylacrylate-Acrylate Copolymers via the Hydrophobicity of the Alkyl Chain and the Length of the Blocks

Özge Azeri^{1*}, Dennis Schönfeld¹, Uwe Keiderling², Laurence Noirez³, Michael Gradzielski^{1*}

1: Stranski-Laboratorium für Physikalische und Theoretische Chemie, Institut für Chemie, Technische Universität Berlin, D-10623 Berlin, Germany

2: Helmholtz-Zentrum Berlin für Materialien and Energie, 14109 Berlin, Germany

3: Laboratoire Léon Brillouin CEA-CNRS, Université Paris-Saclay, F-91191 Gif-sur-Yvette Cedex, France

*corresponding authors: azeri@campus.tu-berlin.de, michael.gradzielski@tu-berlin.de

Abstract

In this work we prepared amphiphilic copolymers with alkylacrylate as hydrophobic and acrylic acid (AA) as hydrophilic block. The alkyl chain was varied from butyl to dodecyl, thereby varying systematically the polarity of the hydrophobic block and its length was between 20 and 40, while the PAA block had ~ 100 units. Such relatively short amphiphiles should equilibrate quickly and their self-assembly properties were characterized by means of critical micelle concentration (cmc) determination. Static light scattering (SLS) and small angle neutron scattering (SANS) allowed to gain detailed information about how the micellar structure depends on the molecular build-up of the copolymers and the degree of ionization of the PAA block. In particular, the extent of hydrophobicity of the alkylacrylate block and its length determine the tendency for micelle formation and the size of the formed micelles.

Keywords ATRP, Polyacrylate, Self-assembly, Amphiphiles, Small Angle Neutron Scattering

1. Introduction

Amphiphilic block copolymers with a hydrophilic and a hydrophobic block are able to form micelles in aqueous solution and such systems have been studied to quite some extent due to the fact that there is an enormous richness in terms of combining different hydrophilic and hydrophobic blocks[1], where the hydrophilic block for instance can be a polyelectrolyte.[2] Such block copolymer micelles are interesting for a number of applications, such as drug

delivery[3] in nanomedicine [4] or nanolithography [5]. Via the length of the individual blocks one can control the overall size of the aggregates, while their architecture depends mostly on the length ratio of hydrophilic and hydrophobic block[6], [7] and accordingly not only micelles can be formed but also vesicular structures or nanotubes.[8] The assembly properties in general can be rationalised by the packing parameter concept according to which the ratio of the volume v_h of the hydrophobic part and the product of interfacial area a_h (at the interface between hydrophobic and hydrophilic part of the molecule) and the effective length L of the hydrophobic part determine the shape of the formed aggregates.[9] For $p = v_h/(a_h \cdot L)$ smaller $1/3$ one expects for formation of spherical micelles, for $1/3 < p < 1/2$ rodlike micelles, and for larger p values locally planar structures, such as vesicles.

Quite frequently such micelles are stimuli-responsive, for instance if the hydrophilic head group is a polycarboxylate or a polyamine which are switchable with respect to their charge by pH changes in the range of pH 5 to 9.[10], [11] Another requirement is that the hydrophobic blocks are not too long and must be in a fluid state, as for systems below the glass transition temperature typically static micelles are observed, as for the case of polystyrene where no response to a solvent change was observed.[12] Such responsiveness together with the ability to incorporate payloads of drugs makes block copolymer micelles also attractive as tunable delivery vehicles for nanomedicine applications as reviewed recently.[4], [13]

Of course, when considering block copolymer micelles for solubilization and delivery purposes it is very important to have a hydrophobic domain, whose polarity can be tuned as often interesting solubilisates (e. g. drug molecules) are of intermediate polarity, and then the hydrophobic block has to be adapted to them. Accordingly, in our work we were interested in synthesising well-defined amphiphilic copolymers with a hydrophobic core of alkyl acrylate, where the extent of hydrophobicity was varied via the alkyl chain, and polyacrylic acid (PAA) as hydrophilic head group and subsequently studying their aggregation behaviour in aqueous solution. The alkyl chain was changed from butyl over hexyl to dodecyl, thereby systematically varying the extent of hydrophobicity. It might be noted that a similar system of poly(*n*-butyl acrylate)-*b*-poly(acrylic acid) has been studied before for longer PnBA chains and in this study relatively monodisperse micelles had been reported that are relatively robust against changes of external parameters like pH or salinity.[14] In our investigation the hydrophobic block was varied from 20-40 units in order to elucidate the effect of the block length but keeping the length short in order to avoid the appearance of kinetically frozen micelles, as they have for instance been reported for longer poly(*n*-butyl acrylate) (PnBA) micelles.[15] However, in general it

was kept rather short in order to be able to form rather dynamic micellar assemblies with these polymer surfactants. These copolymer micelles formed in aqueous solution were studied in structural detail by means of static light scattering (SLS) and small angle neutron scattering (SANS) as a function of copolymer type, concentration and degree of ionization.

2. Materials and Methods

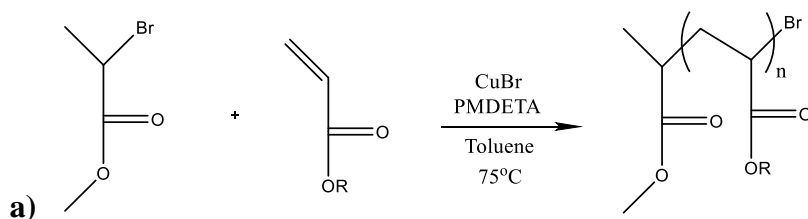
2.1. Materials and Synthesis

2.1.1. Materials

Toluene (>99.5%) from Fluka, methyl-2-bromopropionate (2-MBP, 98%) and hexane from Aldrich, N,N,N',N'',N''-Pentamethyldiethylenetriamine (PMDETA, 99%), hexyl acrylate (98%), dodecyl acrylate (technical grade 90%) from Sigma-Aldrich and diethylether (>99,5%) from Carl-Roth were used as supplied. t-Butylacrylate, n-butylacrylate and dichloromethane were gifts from BASF and used as supplied. Milli-Q water was produced by a Millipore filtering system. D₂O was from Eurisotop (99.5% isotopic purity, Gif-sur-Yvette, France), sodium hydroxide (99%) and sodium chloride (>99%) were obtained from Sigma-Aldrich. Silica (0.04-0.063 mm) from Merck was used for columns. Trifluoroacetic acid (>99.9%) was from Roth.

2.1.2. Synthesis

The synthetic procedure was the same for all samples (depicted in Fig.1), where one begins with the polymerisation of the first monomers to yield a macroinitiator for atom transfer radical polymerization (ATRP). In the next step, this macroinitiator was then used for further polymerisation of t-butyl acrylate via the functional halide group that the polymer carries due to the chosen ATRP mechanism. The formed n-alkyl acrylate-t-butyl acrylate block copolymer was an intermediate product that was transformed to the final product by selective hydrolysis of the t-butyl groups, which was done by reacting with an excess of trifluoroacetic acid (TFA).



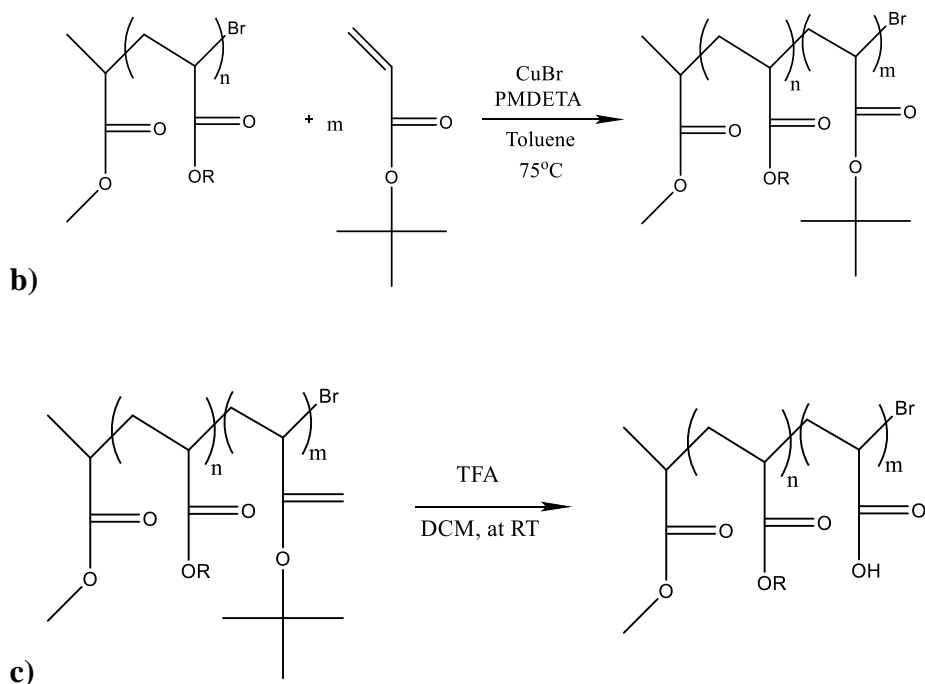


*Figure 1 Synthetic steps to prepare the poly(alkylacrylate)-*b*-poly(acrylic acid) block copolymers by the ATRP procedure. a) polymerization of the alkylacrylate block; b) polymerization of the *t*-butyl acrylate block; intermediate product; c) hydrolysis of the intermediate product to yield the final product*

In particular, in a 100 ml single-neck flask with stirrer, Cu(I)Br and the *n*-alkyl monomer were weighted in. Subsequently, about 40 ml toluene as solvent was added, the flask was closed with a septum and degassed while stirring for 20 min under nitrogen gas. After removal of the oxygen via bubbling with inert gas, first 2-MBP and then PMDETA were added into the reaction medium. The temperature of the oil bath was adjusted to 75 °C. The conversion was checked by means of ¹H-NMR. After about 24 hours, the macroinitiator was ready. The intermediate block copolymer consisting of poly(alkylacrylate)-*b*-poly(*t*-butylacrylate) was synthesized in a one-pot reaction was performed. First, *tert*-butyl acrylate was added into a 50 mL single-neck flask with stirrer and closed with a septum before stirring and degassing for 20 min. CuBr and toluene were placed in another 50 mL one-necked flask and degassed. PMDETA was injected into the flask with CuBr. After dissolving the CuBr owing to complexation of ligand and metal salt, the degassed *tert*-butyl acrylate and ligand-metal complex were transferred via cannula to the flask containing macroinitiator. The conversion of the reaction was checked via ¹H NMR and when the desired conversion was reached, the reaction was stopped by cooling down to ambient temperature and opening the flask. Next, the copper complex was removed by column chromatography with silica as a stationary phase and dichloromethane as eluent.

Finally, the hydrolysis of *tert*-butyl group was performed with trifluoroacetic acid (TFA) for 96 h while stirring at 40 °C in dichloromethane to obtain a final product of polyacrylic acid.

NMR was used to control the progress of the hydrolysis through checking to vanish the peak from tert-butyl group. When the hydrolysis was complete, the reaction was stopped via cooling down the reaction medium. Excess amount of TFA was evaporated under vacuum and the residue was washed with hexane and then diethyl ether to get the final product.

The obtained different types of block copolymers are depicted in Fig. 2.

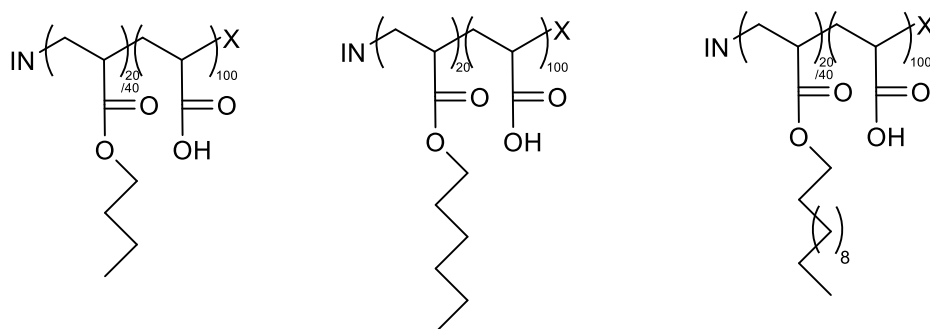


Figure 2 The different types of polymers synthesised: poly(butyl acrylate)-*b*-poly(acrylic acid), poly(hexyl acrylate)-*b*-poly(acrylic acid), and poly(dodecyl acrylate)-*b*-poly(acrylic acid).

The pH-dependency of synthesized polymers was investigated via pH titration. A certain amount of polymer was dissolved in water and NaOH was added into the solution to deprotonate it completely. During the titration with 0.1 M HCl, the excess of NaOH was neutralized first and then polymer had become protonated.

The degree of deprotonation α can be defined as

$$\alpha = \frac{n(OH^-)}{n(AA)}$$

where $n(OH^-)$ are the total moles of added NaOH and $n(AA)$ the moles of acrylic acid units (not taking into consideration whether they are actually protonated or not). This value for acrylic acid/ the chargeable groups was used for the characterization of the synthesized polymers in further analysis.

Characterization of the Polymers

The above-synthesized copolymers then become analyzed with respect to their molecular build-up. In a first step, this was done by NMR on the intermediate product that still contains the t-butyl acrylate (t-Bu) units, as here the signal of the t-Bu groups yields just one sharp singlet which can be well distinguished from the signals from the alkyl groups. These measurements were done in D₂-dichloromethane as solvent with a Bruker Avance II 400MHz instrument at room temperature. Taking into account the molecular formula of the corresponding building

blocks one can then directly calculate the relative content of hydrophobic and hydrophilic block (for details see SI). The obtained values for the six different copolymers are summarised in Table 1 and compared with the values theoretically expected from the amounts of monomer employed in the synthesis procedure. In general, we find good agreement, but especially for the case of the dodecyl acrylate containing copolymers, also a significantly higher content of this hydrophobic block compared to the expected values.

Table 1 Relative molar content of hydrophobic and hydrophilic block according to the NMR spectra compared to the theoretically expected value.

theor. formula	Theoretical		NMR	
	Hydrophobic	Hydrophilic	Hydrophobic	Hydrophilic
nBu ₄₀ -b-PAA ₁₀₀	29%	71%	28.77%	71,23%
nBu ₂₀ -b-PAA ₁₀₀	20%	80%	16.71%	83,29%
nDo ₂₀ -b-PAA ₁₀₀	22%	78%	16.78%	83,22%
nDo ₄₀ -b-PAA ₁₀₀	34%	66%	28.81%	71,19%
nHex ₂₀ -b-PAA ₁₀₀	18%	82%	16.82%	83,18%

The number and weight average molecular weight and weight distribution of non-hydrolysed polymers were determined via gel permeation chromatography (GPC) using THF as eluent with a flow rate of 0.5 ml per minute at 25 °C (the GPC curves are shown in the SI). The GPC is home-made with an isocratic pump and an autosampler (both from Thermo / Finnigan), a 3 µm particle diameter front & 3 µm particle diameter separation column (from PSS), as well as a refractive index detector (Wyatt Optilab DSP). The reference substance was a narrow distribution polystyrene standard.

Table 2: Theoretical molecular weight M_{th} , yield, number average of the molecular weight (M_n) of hydrolyzed polymer, polydispersity index (PDI) from GPC experiments, and the experimentally determined chemical formula of the produced polymers

theor. formula	M_{th} [g/mol]	Yield	M_n [g/mol]	PDI	exp. formula
nBu ₄₀ -b-tBuA ₁₀₀	18871	73 %	20681	1.19	nBu ₆₀ -b-AA ₁₆₇
nBu ₂₀ -b-tBuA ₁₀₀	15904	58 %	16896	1.15	nBu ₃₅ -b-AA ₁₇₂
nDo ₂₀ -b-tBuA ₁₀₀	17347	56 %	17291	1.20	nDo ₃₁ -b-AA ₁₃₇
nDo ₄₀ -b-tBuA ₁₀₀	23371	68 %	13497	1.28	nDo ₃₂ -b-AA ₇₉
nHex ₂₀ -b-tBuA ₁₀₀	16660	71 %	17625	1.12	nHex ₃₃ -b-AA ₁₇₅

Further information regarding the polymer composition was obtained via pH-titration and the M_n and M_w results from GPC was shown in Table S.

2.2. Methods of Colloidal Characterisation

The determination of the critical micelle concentration (cmc) was done by the fluorescence method.[16] For that purpose a NaOH stock solution was used in order to adjust the degree of deprotonation as 0.2 and 1.0 (actually there was 20% excess of NaOH added for the 1.0 solutions in order to ensure complete deprotonation). The weight percentage of polymer stock solutions was 10 g/L for both the degree of deprotonation. The polymer stock solutions were then diluted to 11 different concentrations down to 0.00005 g/L using the pyrene stock solution.

Steady state fluorescence spectra of pyrene were recorded with a Hitachi F-4500 Fluorescence Spectrometer at 25 °C from 350.0 to 420.0 nm after excitation at 334.0 nm. The slit width was set to 5.0 nm for both excitation and emission. For the experiments, a pyrene stock solution was prepared with a pyrene concentration of 5×10^{-8} mol/L.

The pH-titrations were performed at room temperature via a Titrand System with the Software tiamo™ by Metrohm.

Static light scattering (SLS) experiments were carried out with a CGS-3 (compact goniometer system) with a HeNe-Laser at 632.8 nm wavelength and using a hardware V.1.7.0 correlator ALV / LSE-5004 Light Scattering electronic and Multiple Tau Digital Correlator from ALV GmbH (Langen, Germany). Two avalanche photodiodes (APD) were used to detect the scattered light by a pseudo-cross-correlation at various angles between 40-140°.

The SLS intensity for particles should have an angular dependence according to Guinier's law:

$$I(q) = I(0) \cdot \exp(-R_g^2 \cdot q^2 / 2) \quad \text{eq. 1}$$

where R_g is the radius of gyration and q the modulus of the scattering vector ($= 4\pi n_0 \sin(\theta/2)/\lambda$; with n_0 the refractive index of the solvent, θ the scattering angle, and λ the wavelength of the light). From the intensity at zero angle, $I(0)$ one can, via the optical constant K , directly calculate the mass-averaged molecular weight M_w :

$$M_w = I(0) / c \cdot K \quad \text{eq. 2}$$

$$K = 4 \frac{\pi^2 \cdot n_0^2 \cdot (dn/dc)^2}{N_{Av} \cdot \lambda^4} \quad \text{eq. 3}$$

where dn/dc is the refractive index increment and N_{Av} the Avogadro constant.

SANS measurements were performed at PA20 from the Laboratoire Léon Brillouin (LLB, Saclay, France). Three configurations were used (1.9, 8.3 and 18.8 m sample-to-detector

distances) with a wavelength of 6 Å neutrons and also tested a very low q configuration at 18.8 m with 15 Å wavelength for two representative samples. In order to reach higher q , we used an off-centered detector position at the shortest detector distance, 1.9 m. Transmission values were measured in this configuration, in agreement with the existing measurement procedures (scripts) available at the instrument.

Some additional SANS measurements were performed on the V4 instrument at the Helmholtz Zentrum Berlin (HZB). The samples were measured at wavelengths of 7 Å with sample to detector distances of 7 m and collimation length of 7 m respectively.

The scattering of the empty cell was subtracted as background before radial averaging and taking into account the transmissions the differential cross-sections were calculated. Subsequently the data sets obtained for the three different configurations were merged. Finally a constant background from the incoherent scattering was subtracted by extrapolating the intensity at large q by Porod's law.

3. RESULTS AND DISCUSSION

3.1 Critical Micellar Concentration (CMC)

A quantity of central importance to the self-assembly properties of amphiphilic copolymers in aqueous solution is their cmc. The cmc was determined by means of the fluorescence method where 0.05 μM pyrene was employed as a probe molecule and fluorescence spectra measured (details are described in 2.2) in the copolymer concentration range of 50 μg/L to 5 g/L are given in Fig. S. Below the cmc the pyrene has to be located within the aqueous solution, while above it will with large preference be contained in the hydrophobic core of the copolymer micelles. This leads to a change of the fluorescence spectra, as for instance seen in the changing ratio of the first and third emission maximum (I_1/I_3).^[17] From the ratio I_1/I_3 as a function of concentration one can determine the cmc. An example of such a plot is given in Fig. 3 (the remaining such data sets are plotted in Figs. S). The sigmoidal shape of the data sets was described by a Boltzmann-function:

$$\frac{I_1}{I_3} = I_{1/3f} + \frac{I_{1/3i} - I_{1/3f}}{1 + \exp((c - \text{cmc})/\Delta \text{cmc})} \quad \text{eq. 4}$$

with $I_{1/3i}$ and $I_{1/3f}$ being the initial (in pure water) and final ratio (presumably all in the micelles), c is the copolymer concentration, and Δcmc a measure for the width of the micellar transition

regime. The cmc then is the inflection point of these curves. The obtained cmc values are summarised in Table 2 and show only about a factor 20 difference between the most strongly hydrophobic polymer at lowest charging (40% C12, $\alpha = 0.2$) and the least hydrophobic polymer at highest charging (20% C4, $\alpha = 1.0$). It is interesting to note that the cmc becomes systematically lower with the increasing length of the alkyl modification but depends only little on the block length.

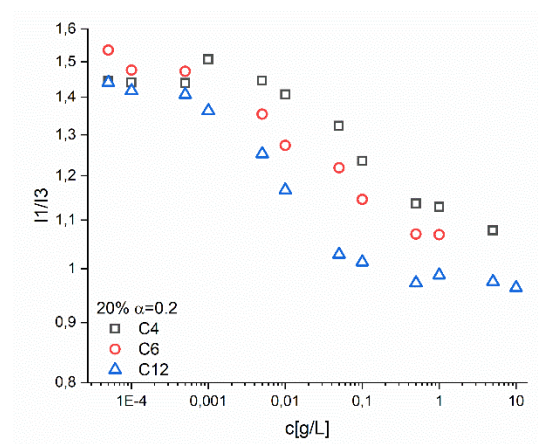


Figure 3 Ratio of the first and third maximum of the emission spectrum of pyrene as a function of concentration for the C4, C6, and C12 copolymer with DP = 20 and $\alpha = 0.2$ ($T = 25$ °C).

The change in Gibbs free energy (ΔG_{mic}) is calculated from the CMC data from the following equation

$$\Delta G_{mic} = RT \ln x_{CMC} \quad \text{eq. 5}$$

Where x_{CMC} is the critical micelle concentration expressed as mole fraction; T is the absolute temperature, and R is the gas constant.

Table 3 cmc in g/L and M, as well as the corresponding free energy of micellization ΔG_{mic} for the different polymers at different degrees of ionization α at 25 °C.

moiety	content	α	cmc [g/L]	cmc [M]	ΔG_{mic} [kJ/mol]
C4	20	0.2	0.0826	4.76E-06	-40.33
	20	1.0	0.1129	6.51E-06	-39.55
	40	0.2	0.0260	1.24E-06	-43.66
	40	1.0	0.0845	4.04E-06	-40.73
C6	20	0.2	0.0168	9.24E-07	-44.39
	20	1.0	0.0252	1.38E-06	-43.39
C12	20	0.2	0.0073	4.06E-07	-46.43
	20	1.0	0.0126	7.00E-07	-45.08

	40	0.2	0.0048	3.41E-07	-46.86
	40	1.0	0.0059	4.20E-07	-46.35

We studied polyacrylic acid-containing polymers with n-butyl, n-hexyl and n-dodecyl alkyl chain as 20% and 40%, to have a systematic variation of the hydrophobicity of polymers. Besides hydrophobicity, pH-dependency was also investigated via changing degrees of ionization α of 0.2 and 1.0 (to make sure about complete deprotonation of the polymer we worked here with an excess amount of NaOH, i.e. α was 1.2 for each fully deprotonated sample). For the structural characterization, static light scattering and small angle neutron scattering experiments were employed, which enables us to understand the mesoscopic organization of different aqueous solutions of synthesized polymer.

Static Light Scattering (SLS)

Static light scattering experiments were performed to gain a first insight into the aggregation behavior of these polymers in aqueous solution. Light scattering experiments were done for four different concentrations as 0.1 wt%, 0.2 wt%, 0.5 wt% and 1.0 wt% with fully deprotonated samples ($\alpha= 1.0$) in order to investigate concentration effect on these systems. Moreover, the samples with a concentration of 0.5 wt% were also prepared for lower ($\alpha=0.2$) deprotonation.

SLS data was evaluated via Guinier plots for all polymers. $I(0)$ values for all samples were obtained from these Guinier plots and M_w were calculated from these $I(0)$ values with using refractive index increment of the polymers as 0.15 ml/g. In particular, as hydrophobicity increases the calculated molecular weight of the aggregates increases as well. The obtained values are summarized in Fig. 4 and Table S1.

The obtained molecular weights for the samples with butyl (40 mol%), hexyl (20 mol%) and dodecyl (40 mol%) moieties are not affected by the concentration of the sample. On the other hand, molecular weights for the samples with butyl (20 mol%) and dodecyl (20 mol%) increase slightly with increasing concentrations. Moreover, samples with dodecyl alkyl chain modification which are the more hydrophobic ones have much higher the molecular weight values compared with other samples.

Furthermore, when the pH-dependency of the systems are compared, it can be noticed that an increase in the degree of ionization has affected on the molecular weight of those systems proportionally. Even though the molecular weights are not significantly differentiated between slightly and fully deprotonation samples, fully deprotonated samples form apparently smaller aggregates than slightly deprotonated ones.

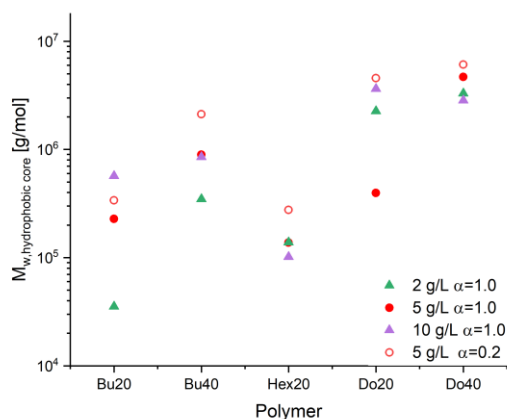


Fig. 4: Molecular weight as a function of the concentration for the different polymers studied ($T = 25\text{ }^{\circ}\text{C}$, $\alpha = 1.0$; one measurement at $\alpha = 0.2$, 5 g/L)

Small-Angle Neutron Scattering (SANS)

Much more detailed information regarding the structure of the micelles formed in aqueous solution can be obtained from SANS experiments, which were done for all block polymers studied and for concentrations of 0.1 wt%, 0.2 wt%, 0.5 wt%, 1.0 wt%. The degree of ionization was $\alpha = 1.0$ for all concentrations and in addition α values of 0.2 and 0.5 for the 0.5 wt% sample. The experiments were performed at HZB on the instrument V4 and LLB on the instrument PA20 and the obtained scattering curves are shown in Fig. 5.

The SANS patterns for almost all samples point to the formation of self-assembled aggregates, only for Bu₃₅-AA₁₇₂ and Hex₃₃-AA₁₇₅ the scattering is so weak and from the pattern may also arise from single polymer molecules. The scattering intensity increases with increasing concentration for all samples (see Fig. S??) When comparing the scattering curves for the polymers with different length of the hydrophobic chain (Fig. ?), it is clearly seen that an increase in alkyl chain length is resulting in an increase of the scattering intensity, and the patterns at the same time are typical for globular aggregates. In other words, polymers with longer alkyl chain modification form bigger aggregates consistently. Even more obvious is the effect of the length of the hydrophobic block, where for the longer blocks much higher scattering intensities are seen. Interestingly for the shorter alkyl chain copolymers, i. e. Bu₃₅-AA₁₇₂, Bu₆₀-AA₁₆₇ and Hex₃₃-AA₁₇₅, one also sees correlation peaks from the electrostatic interaction between the aggregates. This is not seen to the same extent for the dodecyl analogues and this presumably due to the fact that the larger aggregates present there have already PAA chains of the aggregates overlapping in solution and thereby reducing the effective repulsion.

However, the position of the correlation peak around 0.1 nm^{-1} indicates a mean spacing between the aggregates of 50-60 nm, thereby corroborating the presence of aggregates with radii in the range of 20-30 nm.

Further, a comparison for fully $\alpha=1.0$ and little $\alpha=0.2$ deprotonated samples is also interesting to consider the pH dependency of the polymers. The similar samples at full ionization ($\alpha=1.0$) show lower scattering intensities than the corresponding samples at $\alpha=0.2$. The size of the aggregates is getting smaller with increasing the degrees of ionization and this is an effect well to be expected as the more charged head group of the polymeric amphiphile leads to a lower packing parameter and thereby to the formation of smaller aggregates and similar effects have been seen before.[11]

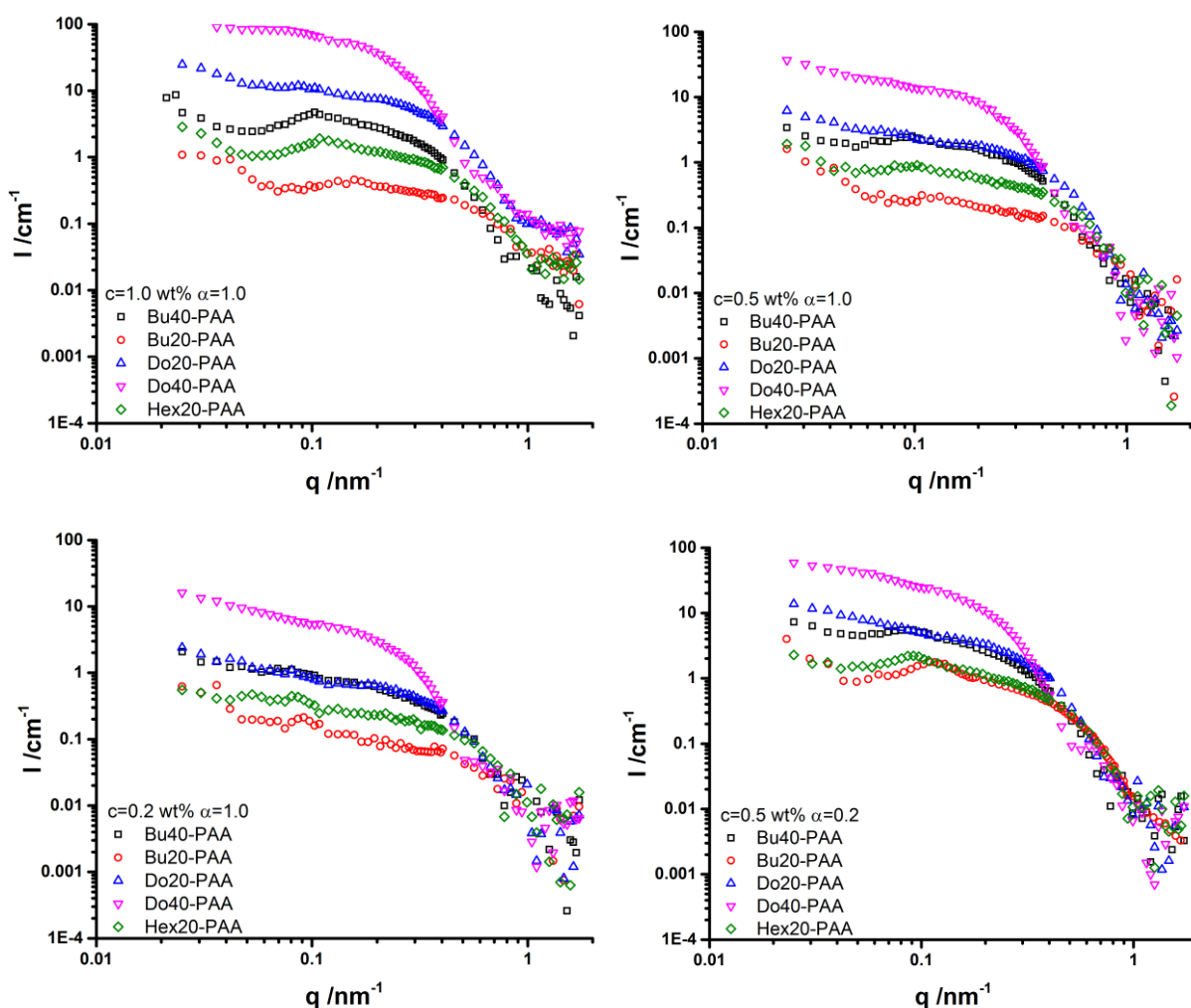


Figure 4 SANS intensity, background corrected, as a function of q for all samples. The samples signed with ** (see Table Sxx) were measured at HZB and all others were measured at LLB.

The results of a model free analysis were summarized in Table S2 and the key parameters molecular weight M_w is shown in Fig. 6 for the variation of the total concentration and in Fig. 7 for the variation of the degree of charging.

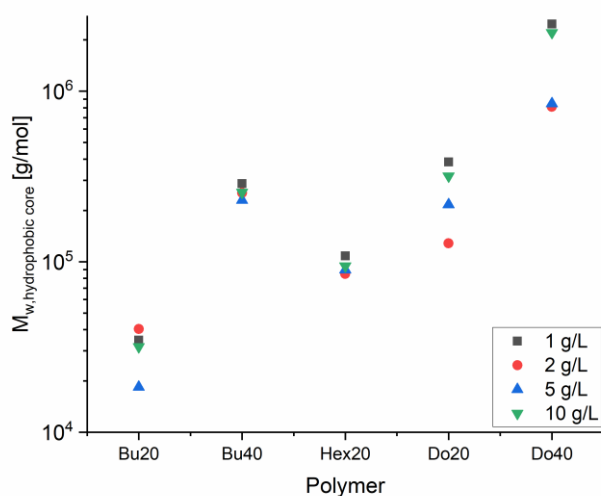


Fig. 6: Molecular weight as a function of the concentration for the different polymers studied ($T = 25\text{ }^\circ\text{C}$, $\alpha = 1.0$).

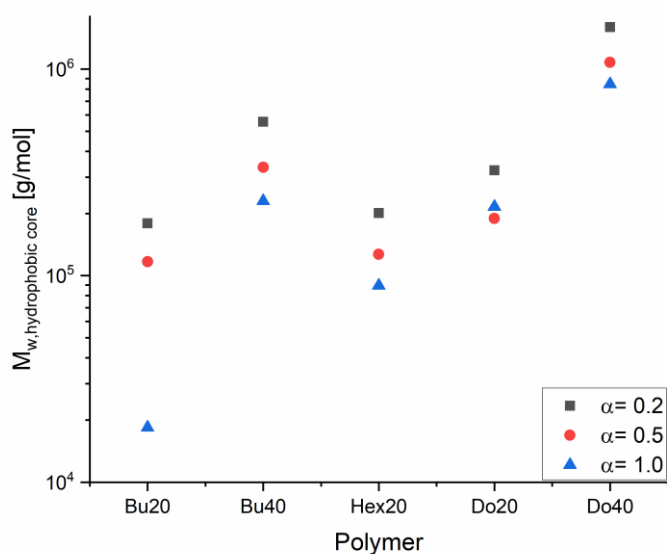


Fig. 7: Molecular weight as a function of the degree of ionization α for the different polymers studied ($T = 25\text{ }^\circ\text{C}$, $c = 5.0\text{ g/L}$).

From these data it becomes evident that Bu20-PAA basically does not aggregate under these conditions and best at highest concentration some very small aggregates are formed. This is substantially changed for Bu20-PAA, where small aggregates with N_{agg} in the range of 7-15 are observed. Interesting the extension of the alkyl chain from butyl to hexyl does have little effect here and for Hex20-PAA also no micellar aggregates are observed. The situation then changes

markedly for the dodecyl case and for Do20-PAA and Do40-PAA even for the lowest concentration and irrespective of the state of ionization globular micelles are observed. However, they are substantially larger by about a factor 8-10 in aggregation number for the longer hydrophobic block. However, this is in good agreement with the expected behaviour if the core size of the micelles is expected to scale with the length of the hydrophobic block.

As a next step, the SANS data was fitted with a model of polydisperse spheres which is formed by the hydrophobic core of synthesized block copolymers. This model is described by eqs (?) and (?), ΔSLD the contrast difference in scattering length densities between the hydrocarbon block and the average of the medium (D_2O), R is the radius of the aggregates and the q magnitude of the scattering vector. LogNormal distribution eq(?) was used to describe the polydispersity of the scattering domains, with the width parameter s , R_m the mean radius, and the number density $N(fp)$ which is expressed as volume fraction fp , that can be defined using the eq(?) and (?). In that formula, $\langle R^3 \rangle$ is the third moment of the LogNorm distribution of the radii.

$$I(q, R_m) = {}^1N(fp) \int_0^\infty \text{LogNorm}(R, N(fp), \sigma, R_m) F(q, R) dR \quad \text{eq. 6}$$

$$F(q, R) = \left(\frac{4\pi R^3 \Delta\text{SLD} (\sin(qR) - qR \cos(qR))}{(qR)^3} \right)^2 \quad \text{eq. 7}$$

$$\text{LogNorm}(R, N(fp), \sigma, R_m) = \frac{N(fp)}{R} \exp\left(\frac{-\ln(R/R_m)^2}{2\sigma^2}\right) \quad \text{eq. 8}$$

$${}^1N(fp) = \frac{fp^3}{4\pi \langle R^3 \rangle} \quad \text{eq. 9}$$

$$\langle R^3 \rangle = R_m^3 \exp\left(\frac{9}{2} \sigma^2\right) \quad \text{eq. 10}$$

We assumed hydrophilic block for the scattering length densities (SLD). Results of scattering data analysis with a model of homogenous sphere (in Table S?), the radius of the aggregates increases with an increasing alkyl chain length. Here it would be worth to be noted data quality is poor due to the low scattering intensities and accordingly corresponding parameters have larger errors. Also, the data with ** were measured at V4-HZB, Berlin

Conclusions

??

Acknowledgments

The authors are grateful to Anja Hörrmann for data reduction, to the Helmholtz-Zentrum Berlin für Materialien und Energie GmbH (HZB, Berlin, Germany) and the Laboratoire Léon Brillouin (LLB, Saclay, France) for allocation of SANS beam time, and to Research group of Prof. Schlaad from University of Potsdam for performing the GPC measurements.

References

- [1] J.-F. Gohy, “Block Copolymer Micelles BT - Block Copolymers II,” V. Abetz, Ed. Berlin, Heidelberg: Springer Berlin Heidelberg, 2005, pp. 65–136.
- [2] S. Förster, V. Abetz, and A. H. E. Müller, “Polyelectrolyte Block Copolymer Micelles,” in *Polyelectrolytes with Defined Molecular Architecture II*, vol. 166, 2004, pp. 173–210.
- [3] K. Kataoka, A. Harada, and Y. Nagasaki, “Block copolymer micelles for drug delivery: Design, characterization and biological significance,” *Adv. Drug Deliv. Rev.*, vol. 64, no. SUPPL., pp. 37–48, 2012.
- [4] H. Cabral, K. Miyata, K. Osada, and K. Kataoka, “Block Copolymer Micelles in Nanomedicine Applications,” *Chem. Rev.*, vol. 118, no. 14, pp. 6844–6892, 2018.
- [5] R. Glass, M. Möller, and J. P. Spatz, “Block copolymer micelle nanolithography,” *Nanotechnology*, vol. 14, no. 10, pp. 1153–1160, 2003.
- [6] H. Shen and A. Eisenberg, “Control of architecture in block-copolymer vesicles,” *Angew. Chemie - Int. Ed.*, vol. 39, no. 18, pp. 3310–3312, 2000.
- [7] C. Fernyhough, A. J. Ryan, and G. Battaglia, “PH controlled assembly of a polybutadiene-poly(methacrylic acid) copolymer in water: Packing considerations and kinetic limitations,” *Soft Matter*, vol. 5, no. 8, pp. 1674–1682, 2009.
- [8] I. W. Hamley, “Nanoshells and nanotubes from block copolymers,” *Soft Matter*, vol. 1, no. 1, pp. 36–43, 2005.
- [9] J. N. Israelachvili, D. J. Mitchell, and B. W. Ninham, “Theory of self-assembly of lipid bilayers and vesicles,” *BBA - Biomembr.*, vol. 470, no. 2, pp. 185–201, 1977.
- [10] E. R. Gillies and J. M. J. Fréchet, “Development of acid-sensitive copolymer micelles

- for drug delivery,” *Pure Appl. Chem.*, vol. 76, no. 7–8, pp. 1295–1307, 2004.
- [11] M. Burkhardt *et al.*, “Polyisobutylene-block-poly(methacrylic acid) diblock copolymers: Self-assembly in aqueous media,” *Langmuir*, vol. 23, no. 26, pp. 12864–12874, 2007.
- [12] P. Hickl, M. Ballauff, and A. Jada, “Small-angle X-ray contrast-variation study of micelles formed by poly(styrene)-poly(ethylene oxide) block copolymers in aqueous solution,” *Macromolecules*, vol. 29, no. 11, pp. 4006–4014, 1996.
- [13] M. E. Fox, F. C. Szoka, and J. M. J. Fréchet, “Soluble polymer carriers for the treatment of cancer: The importance of molecular architecture,” *Acc. Chem. Res.*, vol. 42, no. 8, pp. 1141–1151, 2009.
- [14] O. Colombani, M. Ruppel, F. Schubert, H. Zettl, D. V. Pergushov, and A. H. E. Müller, “Synthesis of Poly(n-butyl acrylate)- block -poly(acrylic acid) Diblock Copolymers by ATRP and Their Micellization in Water,” *Macromolecules*, vol. 40, no. 12, pp. 4338–4350, Jun. 2007.
- [15] P. D. Petrov, M. Drechsler, and A. H. E. Müller, “Self-assembly of asymmetric poly(ethylene oxide)-block-poly(n-butyl acrylate) diblock copolymers in aqueous media to unexpected morphologies,” *J. Phys. Chem. B*, vol. 113, no. 13, pp. 4218–4225, 2009.
- [16] C. Zhao, M. a Winnik, and M. D. Croucher, “Fluorescence Probe Techniques Used To Study Micelle Formation in Water-Soluble Block Copolymers,” *Langmuir*, vol. 6, no. 11, pp. 514–516, 1990.
- [17] M. W. C. Zhao, Y. Wang, R. Xu, M. a Winnik, and M. D. Croucher, “Poly(styrene-ethylene oxide) Block Copolymer Micelle Formation in Water: A Fluorescence Probe Study’,” *Macromolecules*, vol. 24, no. cmc, pp. 1033–1040, 1991.

Supplementary Information

1. NMR Measurements

The NMR spectra for the different copolymers taken in D₂-dichloro methane as solvent.

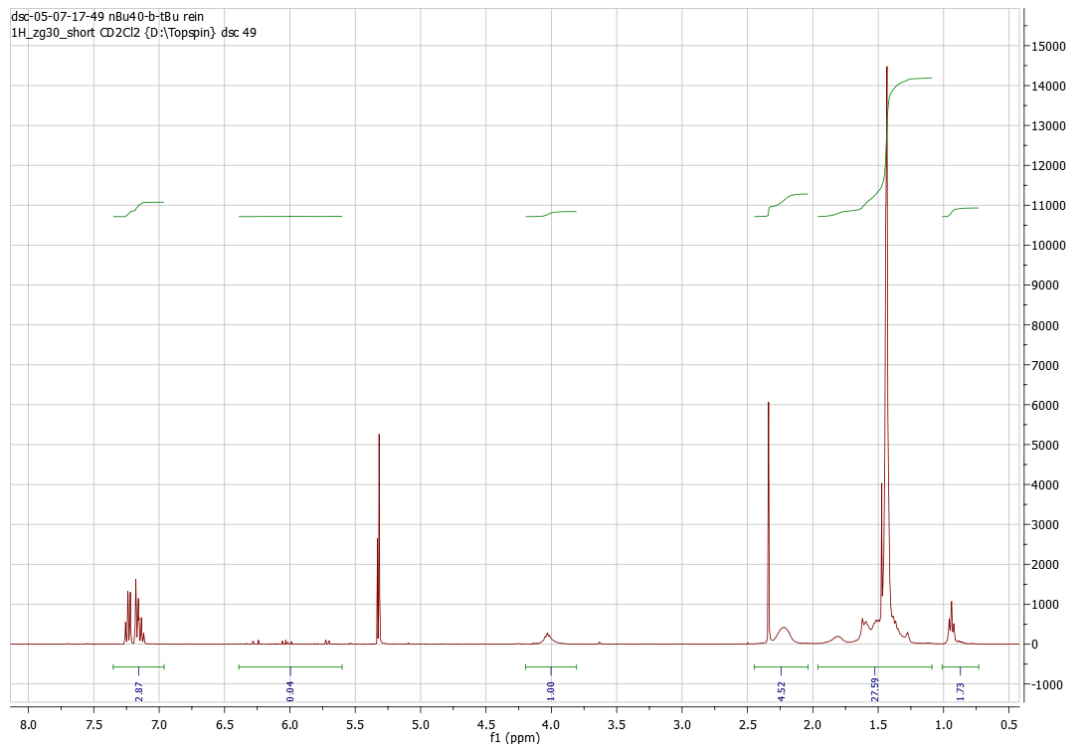


Fig S1 NMR Spectrum of nBu40-b-PAA100

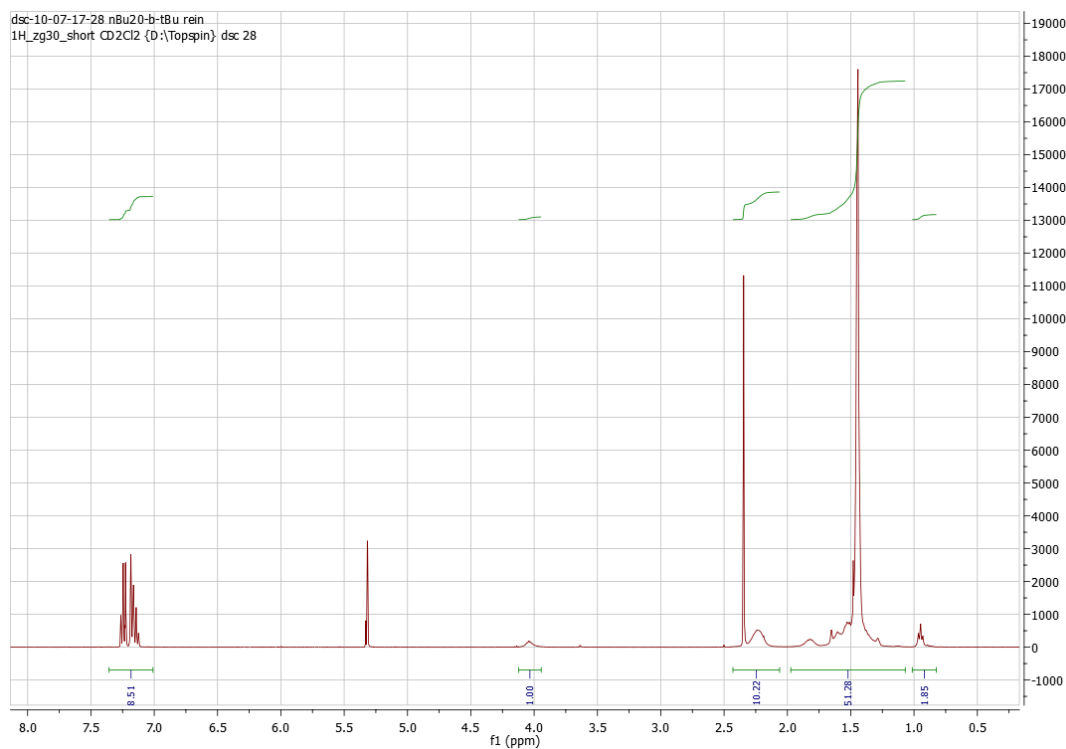


Fig S2 NMR Spectrum of nBu40-b-PAA100

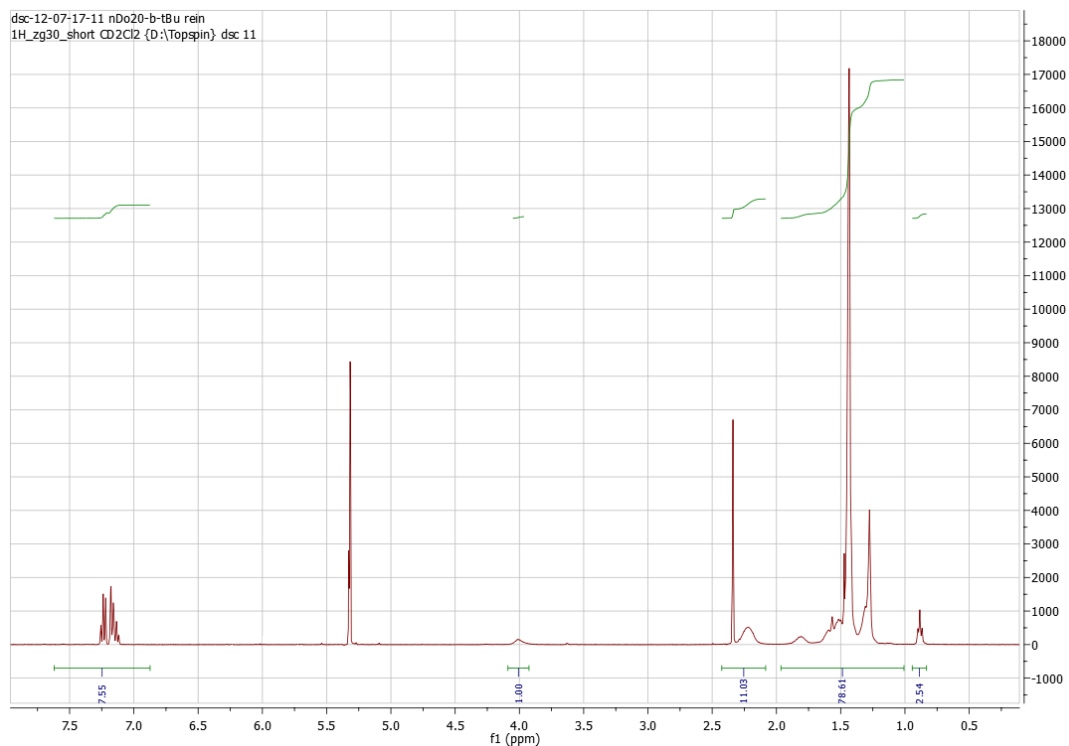


Fig S3 NMR Spectrum of nDo20-b-PAA100

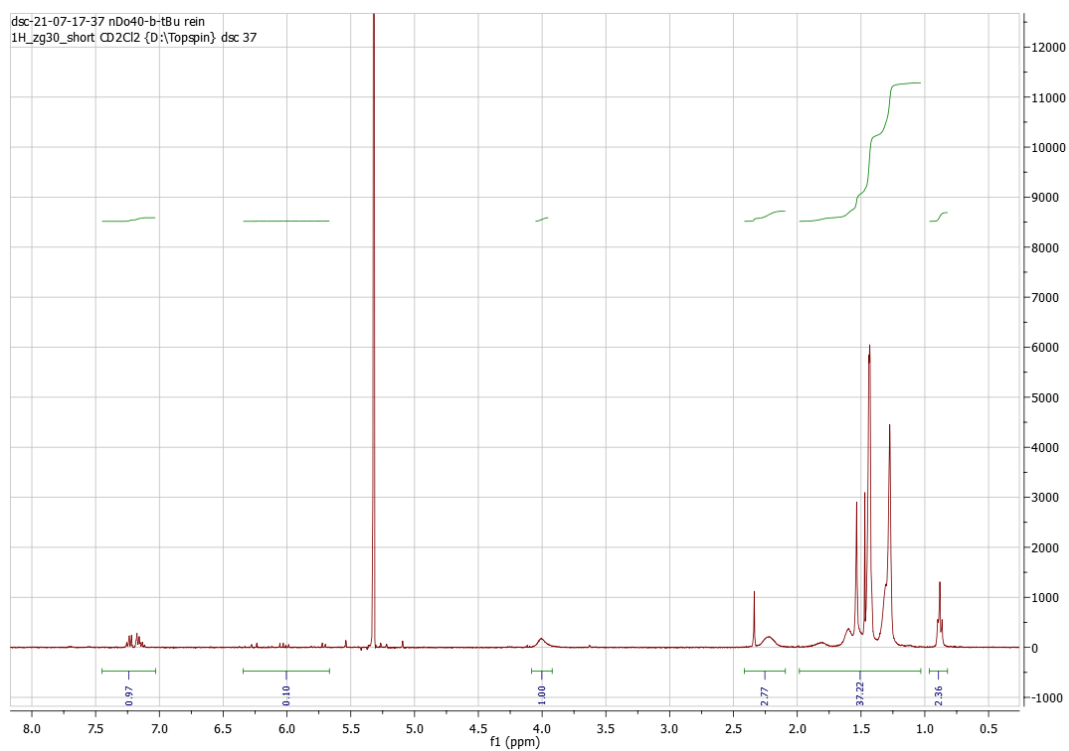


Fig S4 NMR Spectrum of nDo40-b-PAA100

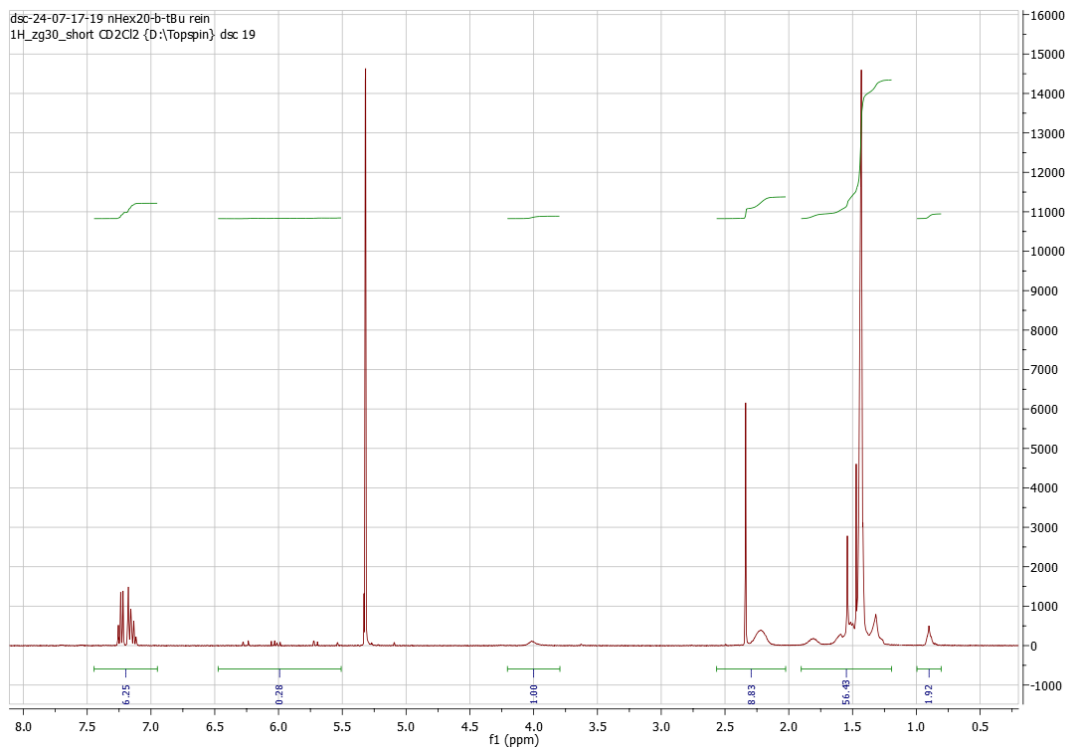


Fig S5 NMR Spectrum of nHex20-b-PAA100

2. Gel Permeation Chromatography (GPC) Measurements

GPC measurements were done in order to determine the molecular weight of the synthesised copolymers and also to gain information regarding the purity of the copolymers.

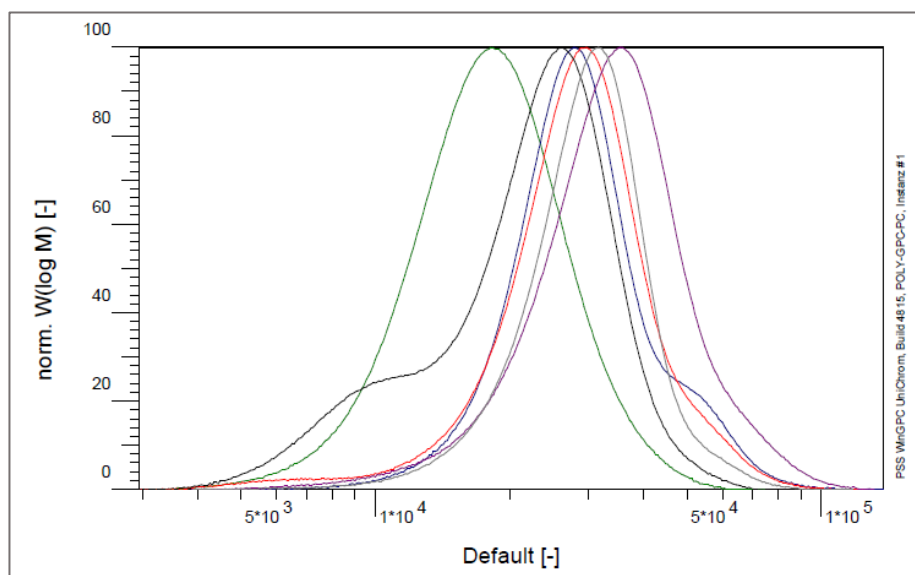


Fig S6 GPC chromatograms for stat. nBu₄₀-tBuA₁₀₀ (green); nBu₂₀-b-tBuA₁₀₀ (blue); nDo₂₀-b-tBuA₁₀₀ (red); nBu₄₀-b-tBuA₁₀₀ (lila); nDo₄₀-b-tBuA₁₀₀ (black); nHex₂₀-b-tBuA₁₀₀ (grey).

Table S1. GPC Results of synthesized polymers

theor. formula	M_n [g/mol]	M_w [g/mol]	PDI
nBu ₄₀ -b-tBuA ₁₀₀	30200 ± 700	36000 ± 800	1.19
nBu ₂₀ -b-tBuA ₁₀₀	26700 ± 500	30600 ± 500	1.15
nDo ₂₀ -b-tBuA ₁₀₀	25100 ± 2400	30100 ± 2900	1.20
nDo ₄₀ -b-tBuA ₁₀₀	18000 ± 500	23000 ± 600	1.28
nHex ₂₀ -b-tBuA ₁₀₀	27600 ± 1700	30900 ± 1900	1.12

3. pH-Titration

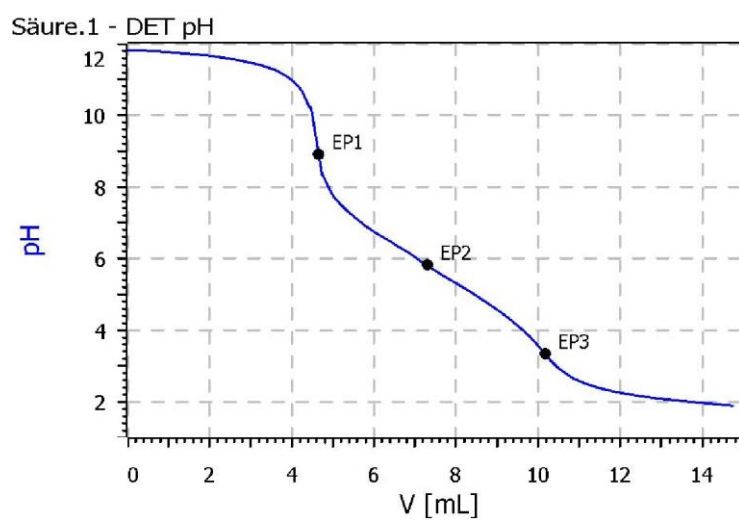
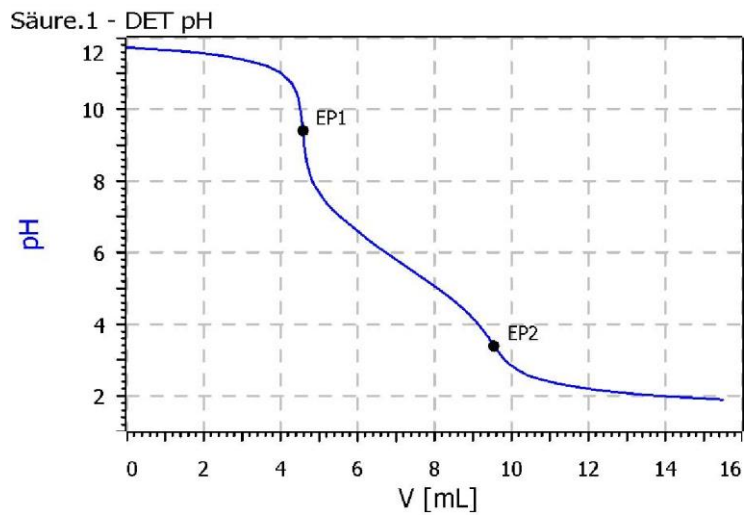


Fig S7 Titration curve of nBu₂₀-b-PAA₁₀₀



Titration curve of nBu40-b-PAA100

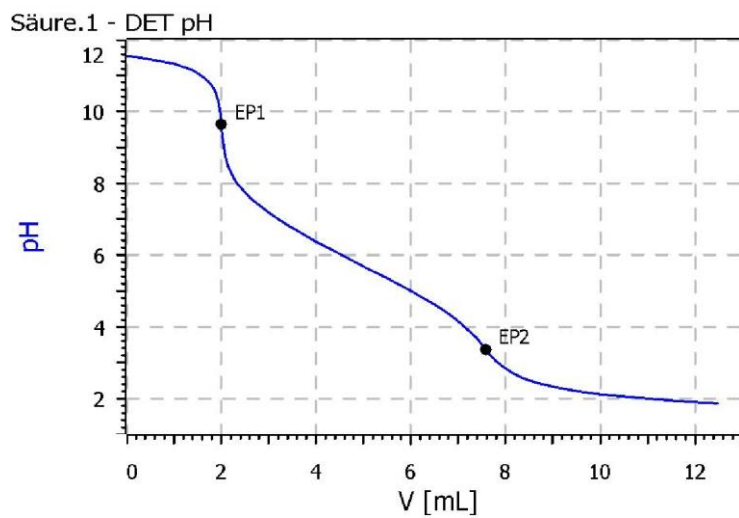


Fig S9. Titration curve of nHex20-b-PAA100

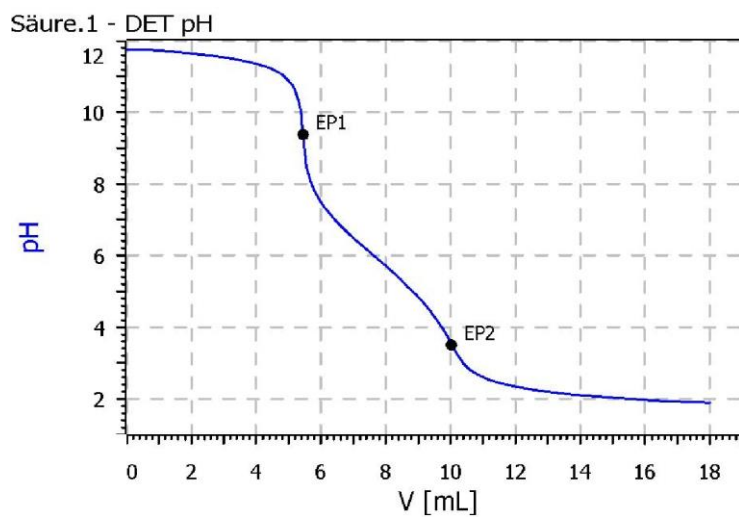


Fig S10. Titration curve of nDo20-b-PAA100

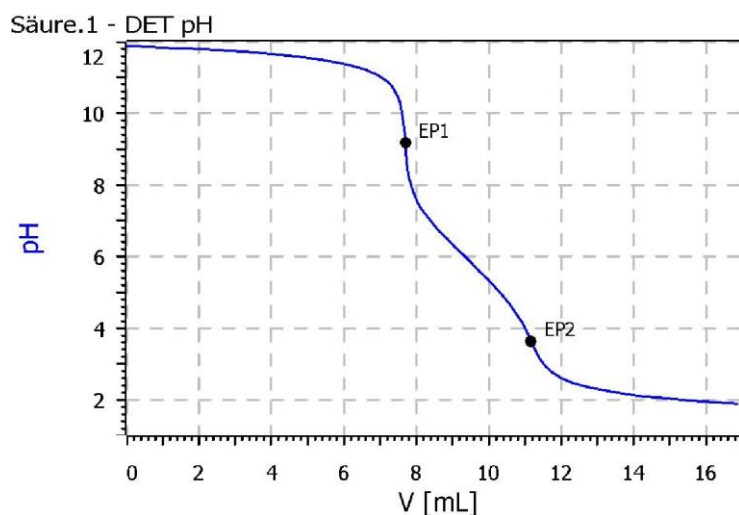


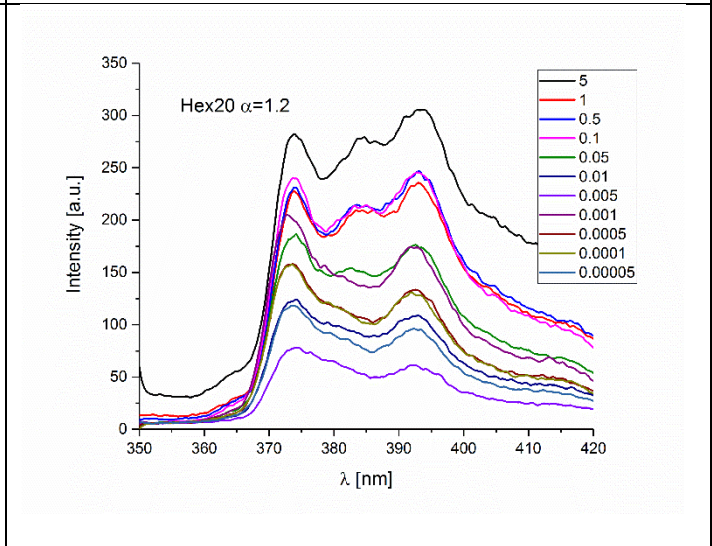
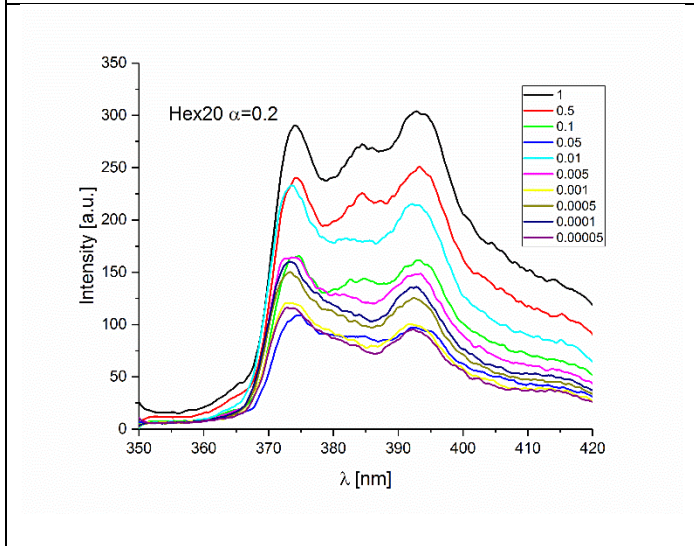
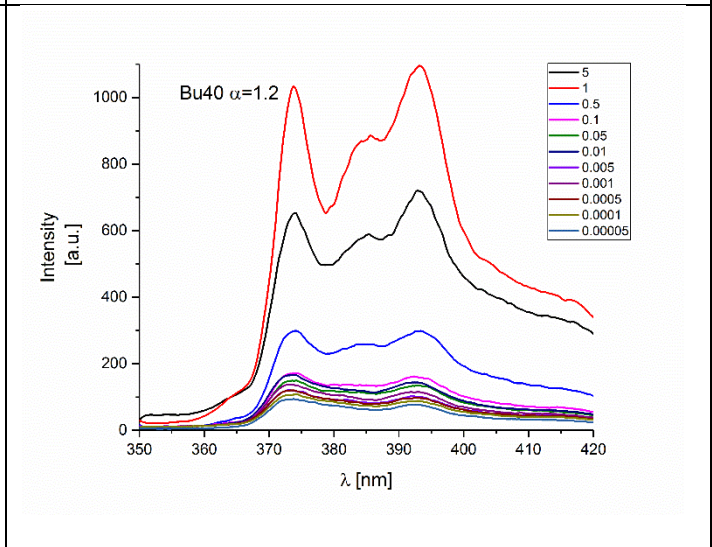
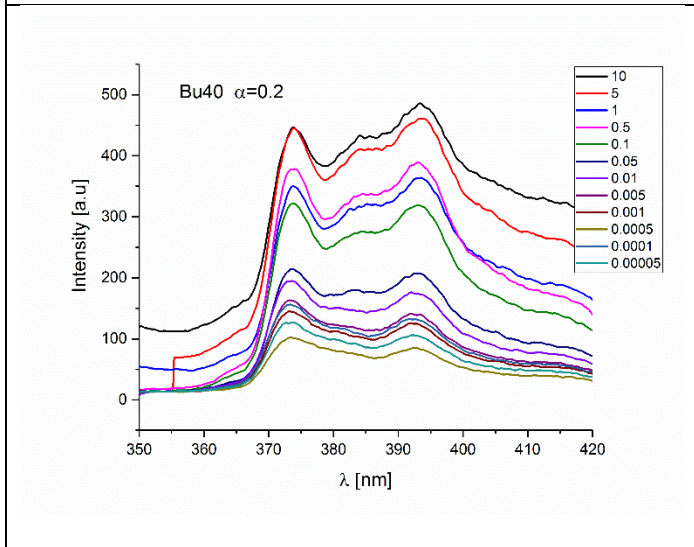
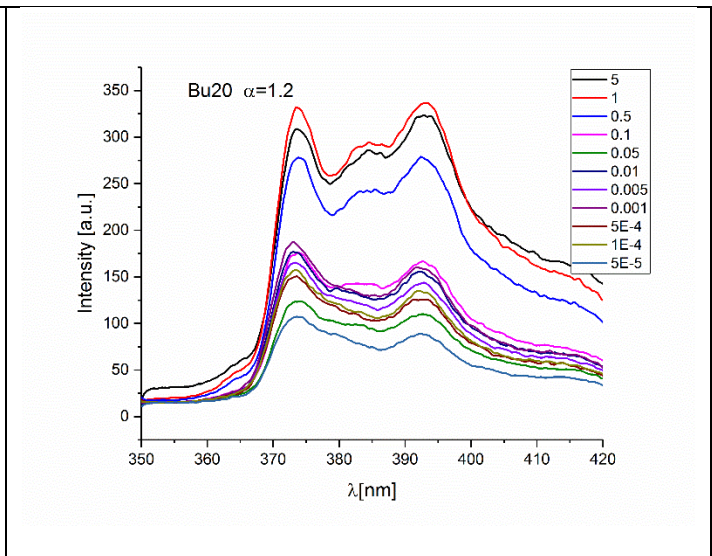
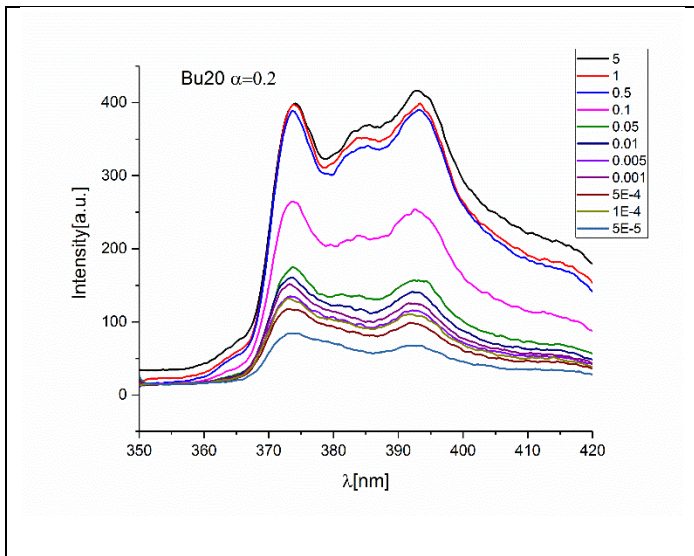
Fig S11. Titration curve of nDo40-b-PAA100

Table S2. Chain Length of the Hydrophobic and Hydrophilic part of the synthesized polymers calculated from pH-titration

theor. formula		Chain Length
nBu40-b-PAA100	Hydrophobic	52
	Hydrophilic	182
	Total	235
nBu20-b-PAA100	Hydrophobic	30
	Hydrophilic	177
	Total	207
nDo20-b-PAA100	Hydrophobic	25
	Hydrophilic	147
	Total	172
nDo40-b-PAA100	Hydrophobic	28
	Hydrophilic	87
	Total	115
nHex20-b-PAA100	Hydrophobic	28
	Hydrophilic	180
	Total	208

3. Fluorescence Spectra

Obtained fluorescence spectra for the different polymers and for different degrees of ionisation are given as a function of concentration in the SI (Figs. ??)



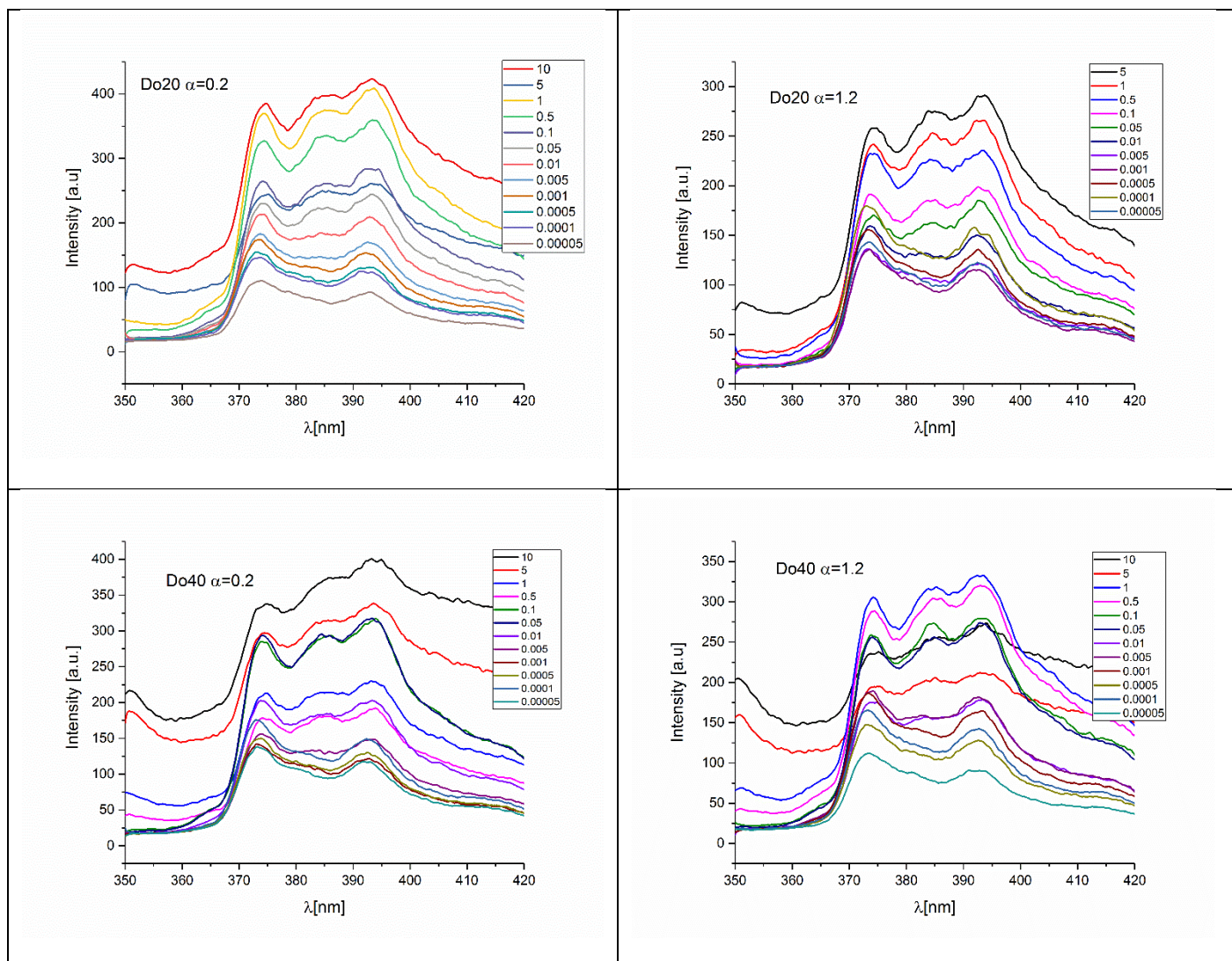


Fig S12. Fluorescence spectra of pyrene in water in the presence of an increasing concentration of block copolymer samples. Concentration c of the samples given in the inset in units of g/L.

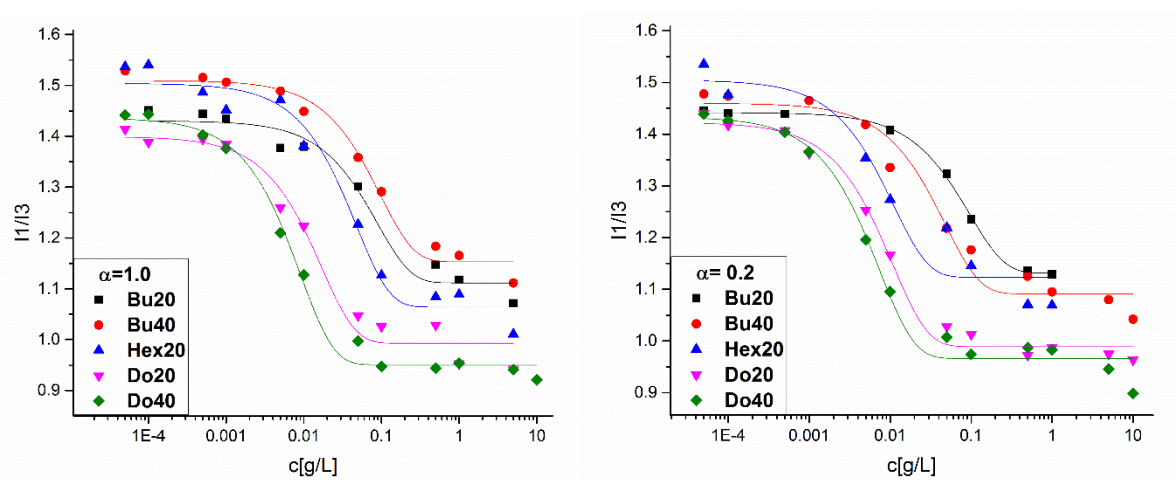


Fig S13. Ratio of the first and third maximum of the emission spectrum of pyrene as a function of concentration for different values of degrees of ionisation at room temperature

4. Static Light Scattering

Table S3 Parameters obtained from the static light scattering experiments. Intensity extrapolated to zero angle, $I(0)$, the molecular weight of scattered object M_w^{app} , the aggregation number, N_{agg} , $M_w^{app,hphobic}$ is the apparent molecular weight of the hydrophobic core, the radius of the hydrophobic core, $R_{hphobic}$.

$$N_{agg} = \frac{M_w^{app}}{M_{w,polymer}}$$

$$M_w^{app,hphobic} = N_{agg} * M_{w,hphobic}$$

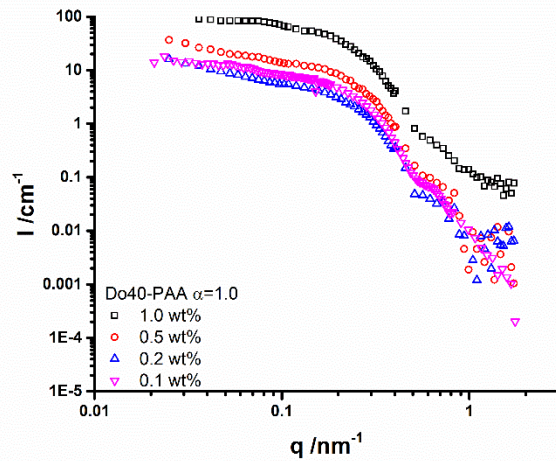
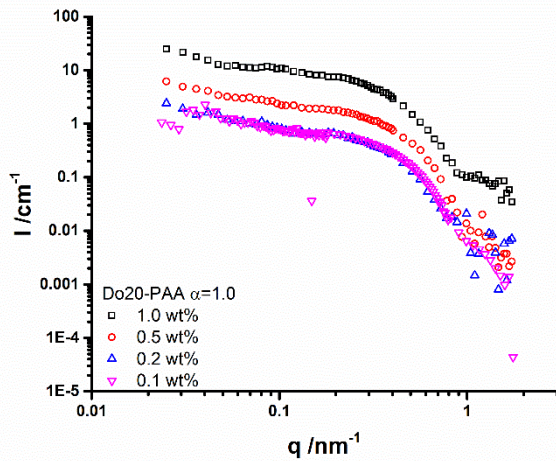
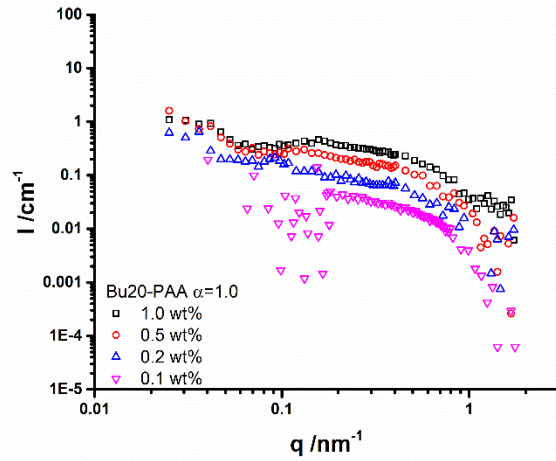
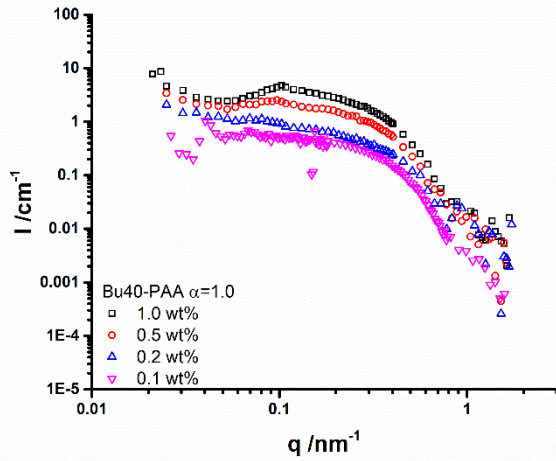
$$R_{hphobic} = \sqrt[3]{\frac{Vp * 3}{4 * \pi}}$$

$$Vp = \frac{M_w^{app,hphobic}}{\rho * N_{av}}$$

Static Light Scattering (SLS)							
	c [g/L]	α	I(0) [1/cm]	M_w^{app} [g/mol]	N_{agg}	$M_w^{app,hphobic}$ [g/mol]	$R_{hphobic}$ [nm]
Bu20	1	1.0	9.24E-05	5.6E+05	33.6	1.50E+05	3.78
	2	1.0	1.09E-04	1.3E+05	7.9	3.53E+04	2.34
	5	1.0	7.02E-04	8.6E+05	51.0	2.28E+05	4.35
	10	1.0	3.50E-03	2.1E+06	127.0	5.69E+05	5.90
	5	0.2	1.04E-03	1.2E+06	75.6	3.39E+05	4.96
Bu40	1	1.0	1.37E-03	8.4E+06	406.5	3.12E+06	10.40
	2	1.0	7.64E-04	9.3E+05	45.4	3.48E+05	5.01
	5	1.0	1.96E-03	2.4E+06	116.4	8.94E+05	6.86
	10	1.0	3.74E-03	2.2E+06	110.9	8.52E+05	6.75
	5	0.2	4.64E-03	5.7E+06	275.8	2.12E+06	9.14
Hex20	1	1.0	5.76E-04	3.5E+06	200.4	1.03E+06	7.19
	2	1.0	3.87E-04	4.7E+05	26.9	1.39E+05	3.68
	5	1.0	3.85E-04	4.7E+05	26.8	1.38E+05	3.68
	10	1.0	5.69E-04	3.4E+05	19.8	1.02E+05	3.32
	5	0.2	1.2E-03	7.3E+05	53.7	2.76E+05	4.64

Do20	1	1.0	1.84E-03	1.1E+07	651.5	4.85E+06	12.04
	2	1.0	4.28E-04	5.2E+06	304.0	2.26E+06	9.34
	5	1.0	7.51E-04	9.2E+05	53.3	3.96E+05	5.23
	10	1.0	1.37E-02	8.4E+06	488.5	3.63E+06	10.94
	5	0.2	8.65E-03	1.0E+07	614.5	4.57E+06	11.81
Do40	1	1.0	4.64E-03	2.8E+07	2110.3	1.62E+07	18.01
	2	1.0	4.66E-03	5.7E+06	430.3	3.30E+06	10.60
	5	1.0	6.70E-03	8.2E+06	609.4	4.68E+06	11.91
	10	1.0	8.15E-03	5.0E+06	370.5	2.85E+06	10.09
	5	0.2	8.71E-03	1.0E+07	792.4	6.09E+06	12.99

5. Small Angle Neutron Scattering (SANS)



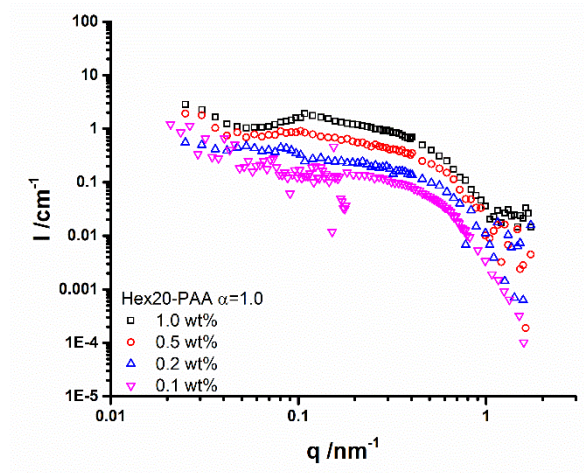


Fig S14. SANS intensity, as a function of the magnitude q of the scattering vector for samples with different concentrations and $\alpha=1.0$

The hydrophobic volume fraction Φ in the samples was calculated according to eq. S..

$$\phi = x_m \left(\frac{a \cdot V_{\text{block}}}{a \cdot V_{\text{block}} + b \cdot V_{\text{block}}} \right) \quad \text{eq. (S.)}$$

with x_m the mass fraction of the polymer, a the length of the hydrophobic chain, b the length of the hydrophilic chain, V_{block} the molecular volume of the corresponding block calculated from SASfit-tools.

Table S2 Mw, Nagg, and R were obtained from model free analysis of SANS data from LLB and HZB which is marked as **. Rg is calculated from Guinier fit.

SANS [LLB] and **[HZB]						
	c [g/L]	α	Mw [g/mol]	Nagg	R [nm]	Rg [nm]
Bu20	1	1.0	3.46E+04	7.7	2.33	3.31**
	2	1.0	4.03E+04	9.0	2.45	3.06
	5	1.0	1.84E+04	4.1	1.89	3.22
	10	1.0	3.17E+04	7.1	2.26	3.07
	5	0.2	1.79E+05	39.9	4.02	4.07
	5	0.5	1.17E+05	26.0	3.49	3.73**
Bu40	1	1.0	2.87E+05	37.4	4.71	4.91**
	2	1.0	2.53E+05	33.0	4.52	5.17
	5	1.0	2.30E+05	30.0	4.38	5.23
	10	1.0	2.55E+05	33.2	4.53	5.47
	5	0.2	5.56E+05	72.4	5.88	6.33
	5	0.5	3.35E+05	43.6	4.96	5.58
Hex20	1	1.0	1.08E+05	20.9	3.46	3.69**
	2	1.0	8.48E+04	16.5	3.20	3.48
	5	1.0	8.95E+04	17.4	3.25	3.86
	10	1.0	9.42E+04	18.3	3.31	4.01
	5	0.2	2.01E+05	39.0	4.26	4.95
	5	0.5	1.27E+05	24.7	3.66	4.34
Do20	1	1.0	3.85E+05	51.8	5.48	4.39**
	2	1.0	1.28E+05	17.2	3.80	4.59
	5	1.0	2.16E+05	29.1	4.52	4.53
	10	1.0	3.18E+05	42.8	5.14	4.73
	5	0.2	3.24E+05	43.6	5.17	5.80
	5	0.5	1.89E+05	25.4	4.32	4.87
Do40	1	1.0	2.48E+06	322.3	10.18	7.67**
	2	1.0	8.10E+05	105.5	7.02	7.67
	5	1.0	8.46E+05	110.1	7.12	7.61
	10	1.0	2.21E+06	287.2	9.80	8.56
	5	0.2	1.60E+06	207.7	8.79	9.27
	5	0.5	1.08E+06	140.8	7.73	8.02

Table S?. Parameters calculated from a spherical model for the samples. Φ is the calculated volume fraction (eq S1) of the hydrophobic core, f_p the volume fraction from the fit, R_m the radius of the hydrophobic core.

Moiety	c [g/L]	α	SANS- Simple spherical model		
			Φ	f_p/Φ	R_m
Bu20	1	1.0	0.00023	0.595	1.92**
Bu20	2	1.0	0.00046	0.308	3.62
Bu20	5	1.0	0.00116	0.425	2.26
Bu20	10	1.0	0.00231	0.329	2.62
Bu20	5	0.2	0.00116	0.737	3.62
Bu20	5	0.5	0.00116	0.672	3.22**
Bu40	1	1.0	0.00035	0.660	4.85**
Bu40	2	1.0	0.00069	0.565	4.02
Bu40	5	1.0	0.00173	0.452	5.03
Bu40	10	1.0	0.00347	0.377	5.38
Bu40	5	0.2	0.00173	0.559	5.67
Bu40	5	0.5	0.00173	0.516	4.89
Hex20	1	1.0	0.00022	0.761	3.42**
Hex20	2	1.0	0.00044	0.707	3.22
Hex20	5	1.0	0.00109	0.636	3.25
Hex20	10	1.0	0.00266	0.435	3.50
Hex20	5	0.2	0.00109	0.736	3.69
Hex20	5	0.5	0.00109	0.591	3.77
Do20	1	1.0	0.00025	1.578	4.39**
Do20	2	1.0	0.00050	0.643	4.85
Do20	5	1.0	0.00125	0.985	4.46
Do20	10	1.0	0.00424	0.941	4.56
Do20	5	0.2	0.00125	0.907	5.55
Do20	5	0.5	0.00125	0.861	4.75
Do40	1	1.0	0.00037	2.395	7.96**
Do40	2	1.0	0.00075	0.796	7.87
Do40	5	1.0	0.00187	0.838	7.89
Do40	10	1.0	0.00568	1.229	7.56
Do40	5	0.2	0.00187	0.914	9.33
Do40	5	0.5	0.00187	0.901	8.46